PERGAMON

Neural Networks 14 (2001) 727–735

Neural Networks

www.elsevier.com/locate/neunet

2001 Special issue

Zero-lag synchronous dynamics in triplets of interconnected cortical areas

D. Chawla, K.J. Friston*, E.D. Lumer

Wellcome Department of Cognitive Neurology, Institute of Neurology, Queen Square, London WC1N 3BG, UK

Received 15 February 2001; accepted 15 February 2001

Abstract

Oscillatory and synchronized activities involving widespread populations of neurons in neocortex are associated with the execution of complex sensorimotor tasks and have been proposed to participate in the 'binding' of sensory attributes during perceptual synthesis. How the brain constructs these coherent firing patterns remains largely unknown. Several mechanisms of intracortical synchronization have been considered, in particular mutual inhibition and reciprocal excitation. These mechanisms fail to account for the zero-lag correlations observed among areas located at different levels in the visual hierarchy because the asymmetric laminar organization of ascending and descending connections in this hierarchy would predict systematic inter-areal phase lags. Here we show through detailed computer simulations that, when triplets rather than pairs of reciprocally connected areas in a cortical hierarchy are considered, zero-lag synchronization emerges naturally from their three-way interactions. These simulations were motivated by the observation that most areas in the cat and macaque monkey visual cortex are organized in such triplets. Our results suggest that patterns of anatomical connections in the mammalian neocortex provide a structural basis for the multi-level synchronization of neuronal activity.

Keywords: Synchrony; Cross-correlogram; Simulations; Cortical hierarchy; Time-lag

1. Introduction

The mammalian visual system comprises a large number of cortical areas dealing with different attributes of the visual scene. A remarkable feature of the connections between these areas is the fact that they exhibit specific patterns of laminar origin and termination. In a well-known proposal, Felleman and Van Essen (1991) organized visual cortical areas in a hierarchy on the basis of these connectivity patterns. Within this hierarchy, ascending connections project from lower to higher-order visual areas and terminate in layer 4. These ascending connections are largely reciprocated by descending projections that terminate outside of layer 4. The organization of visual areas into levels on the basis of these connectivity patterns reflects that observed functionally. Neurons in areas at higher levels in the visual hierarchy exhibit larger receptive field sizes and more complex response properties.

The dense network of ascending and descending connections in the visual hierarchy provides an anatomical basis for the interactions needed to link neuronal processes distributed over widely separated regions into coherent representational states. A robust signature of these multi-stage interactions is the presence of zero-lag synchronization among cortical areas. For example, synchronous firing between parietal area 7 and area 17, as well as between area 7 and motor areas 4 and 5, has been recorded from the cortex of cats engaged in visuomotor tasks (Roelfsema, Engel, Konig & Singer, 1997). Synchrony without time lags has also been observed between visual areas V1 and V2 in awake monkeys (Frien, Elkhorn, Bauer & Wellborn, 1994). Synchronous dynamics among cortical areas is also characteristic of other sensory modalities, suggesting that it represents a fundamental property of cortical interactions. For instance, Nicolelis, Baccala, Lin and Chapin (1995) have found synchronous dynamics across different levels of the rat somatosensory cortex. However, the mechanisms leading to zero-lag synchrony among widely separated areas in a sensory hierarchy are not clear.

Simulations based on realistic neuroanatomical and physiological properties of neuronal architectures suggest that reciprocal interactions between pairs of areas located at different levels in the visual hierarchy would produce systematic lags between their activities. These time-lags reflect the asymmetric laminar specificity of ascending and descending connections between the modeled areas, as the mutual influences that circumscribed populations of cells in two areas exert on each other are mediated through polysynaptic circuits with finite latencies. These time lags increase when the asymmetry between ascending and descending projections is further expressed at the synaptic

* Corresponding author. Tel.: +44-207-833-7457.
E-mail address: k.friston@fil.ion.ucl.ac.uk (K.J. Friston).

0893-6080/01/$ - see front matter
PII: S0893-6080(01)00043-0

level. Indeed, physiological investigations into types of synaptic arbors (Rockland, 1996) have shown ascending inputs to be strong and driving and descending inputs to be weak and modulatory. Consistent with this synaptic asymmetry, visual area V1 has a strong driving effect on the hierarchically higher area V2, in the sense that visual activation of V2 depends on input from V1 (Schiller & Malpeli, 1977; Sandell & Schiller, 1982). This dependency has been demonstrated by reversibly cooling (deactivating) V1 while recording from the retinotopically corresponding region of V2, during visual stimulation (Schiller & Malpeli, 1977; Girard & Bullier, 1989). In contrast, cooling V2 has a more modulatory effect on V1 unit activity (Sandell & Schiller, 1982). The functional asymmetry between V1–V2 interactions has now been established in humans using functional magnetic resonance imaging (Friston, Ungerleider, Jezzard & Turner, 1995). Additionally, there is evidence that V2 has a strong driving effect on V5 while V5 has a more modulatory effect on V2 (Girard & Bullier, 1989). The inter-areal time lags, that result from inter-cortical synaptic asymmetry in simulations, contrast with the in-phase synchronization that is readily produced by monosynaptic, reciprocal interactions between areas occupying the same level in the visual hierarchy. They also contradict the empirical observation of zero-lag synchrony between areas that are separated by several levels in the visual hierarchy.

In this paper, we propose that the discrepancy between physiological and simulated cortical dynamics can be resolved when interactions between more than two interconnected areas are considered. By analyzing the known inter-areal connectivity in the cat and macaque monkey visual cortex, we first show that it exhibits, as a major component of its organization, 'tertiary loops', or sets of connections that reciprocally link triplets of visual cortical areas. Using biologically-based computer simulations, we then show that the three-way interactions among such triplets of areas lead naturally to the emergence of zero-lag dynamics. Finally, we discuss the functional organization of the mammalian neocortex in the light of these new results.

2. Methods

In the first component of this study, we analysed a connectivity matrix between 32 visual areas in the macaque monkey, as given in Felleman and van Essen (1991). This matrix contains information as to which areas are interconnected, and whether connections from one area to another are ascending, descending, or lateral. Specifically, we counted the number of sets of reciprocally connected areas and how many third areas provided common input to each of these pairs.

The second stage of this study focused on the time-lag of synchrony between two or three reciprocally connected cortical areas, each with input from their own thalamic region. Each cortical area was divided into three laminae corresponding to the supra and infragranular layers and layer 4 [Fig. 1(a)]. This laminar organization is consistent with known cortical anatomy (Felleman & van Essen, 1991). Each layer contained 400 excitatory cells and 100 inhibitory cells giving a ratio of inhibitory to excitatory cells that is consistent with experimental results (Beaulieu, Kisvarday, Somogyi & Cynader, 1992). Intra and inter-laminar connection ratios are given in Table 1 and included both excitatory and inhibitory connections (with AMPA and GABAa synapses, respectively). The supragranular cells also expressed modulatory NMDA and slow GABAb synapses. The pattern of inter-layer connections can be seen in Fig. 1(a). GABAb connections were also implemented from the supragranular layer to the other two layers to represent double-bouquet cells. Our ratio of inter-layer/intra-layer connections approximated the 45/28% ratio reported in the cat striate cortex (Lumer et al., 1997a). The thalamic region consisted of one thalamic and one reticular thalamic layer. The thalamic layer had 100 excitatory

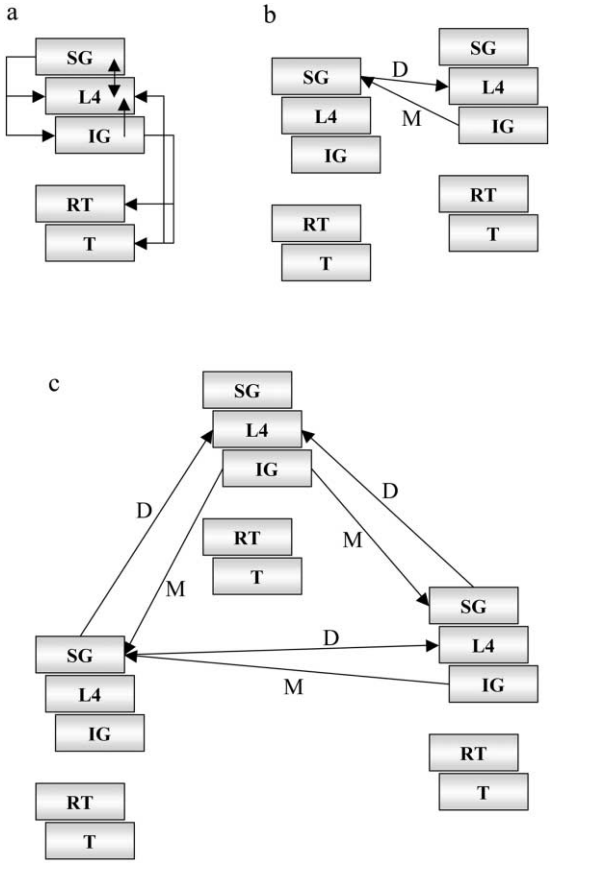

Fig. 1. Architecture of the models studied. (a) A schematic showing the connectivity structure within one thalamo-cortical region. (b) Two thalamo-cortical regions where the first cortical area provides driving input to the second and the second cortical area provides modulatory input to the first. (c) Shows the same as in (b), but with a third area receiving driving input from both areas and providing modulatory input to both areas. In these diagrams SG, L4 and IG refer to supragranular layers, layer 4 and infragranular layers respectively. D and M refer to driving (AMPA) and modulatory (NMDA) connections, respectively.

Table 1
The connectivity ratios in the model

Area(s)	Laminar specificity of connections	Probability of cell projections (%)	Excitatory or inhibitory	Projection synapses
Cortical	Intra-laminar	10	Both	AMPA and GABAa
	Inter-laminar	7.5	Excitatory	AMPA
Thalamus	Intra-laminar	5	Inhibitory	GABAa
	Inter-laminar	5	Inhibitory	GABAa
	Thalamic to reticular layer	5	Excitatory	AMPA
Thalamo–cortical	Thalamic layer of thalamus to layer 4 of cortex (feedforward)	5	Excitatory	AMPA
	Infragranular layer of cortex to thalamic layer of thalamus (feedback)	5	Excitatory	AMPA
Cortico–cortical	Supragranular layer of 1st area to layer 4 of 2nd area	5	Excitatory	AMPA (driving)
	Infragranular layer of 2nd area to supragranular layer of 1st area	5	Excitatory	NMDA (modulatory)

cells and 100 inhibitory cells while the reticular thalamic layer incorporated only 100 inhibitory cells. The anatomy used in this thalamocortical model was consistent with previous simulation studies into neuronal dynamics and has been tested against empirical data (Lumer, Edelman & Tononi, 1997a, b; Sukov & Barth, 1998).

First, only two areas were modeled [Fig. 1(b)]. Feedforward connections between cortical areas were driving and feedback connections were modulatory [Fig. 1(b)]. The synapse to neuron ratio in this model was consistent with experimental findings (Beaulieu & Colonnier, 1983, 1985). Next, a third cortical area, with its own thalamic region, was added to the model [Fig. 1(c)]. This was placed higher in the hierarchy than both of the other cortical areas and, thus, the first two cortical areas projected to this area in a feed forward fashion. In turn they received common modulatory input from the third area. Finally, the third area was modeled as being midway in the cortical hierarchy between the two areas and so provided feedforward input to one area while feeding back to the other area.

Individual neurons, both excitatory and inhibitory, were modeled as single-compartment, integrate and fire units (see Appendix A). Synaptic channels were modeled as fast AMPA and slow NMDA for excitatory and fast GABAa and slow GABAb for inhibitory channels (Stern, Edwards & Sakmann, 1992; Otis and Mody, 1992; Otis, Konick & Mody, 1993). These synaptic influences were modeled using dual exponential functions, with the time constants and reversal potentials taken from the experimental literature (see Lumer et al., 1997a for the use and justification of similar parameters to those used in the present model). Adaptation was implemented in each excitatory cell by simulating a GABAb input from the cell onto itself (Calabresi, Mercuri, Stefani & Bernardi, 1990; Lorenzon & Foehring, 1992). Transmission delays for individual connections were sampled from a non central Gaussian distribution. Intra area delays had a mean of 2 ms and a standard deviation of 1ms. The mean inter-area delays were manipulated throughout this study in order to alter the time-lag of the inter-area synchronous dynamics. The standard deviation of the inter-area delays was always 1 ms. When a third area was implemented in the model (Fig. 4), the mean transmission delay between the third area and the coupled areas was equal to the mean transmission delay between the coupled areas. When the third area had differential transmission delays with the paired areas, the mean transmission delay, averaged over both pathways, from area three to area one and area three to area two, was equal to the transmission delays between the pair of areas. For example when the mean transmission delay between the paired areas was 4 ms, the differential delays between the third area and the two areas were 2 and 6 ms, when the mean delays between coupled areas was 6 ms, the differential delays were 4 and 8 ms and so on. A continuous random noisy input was provided to all thalamic units. In order to manipulate the intrinsic activity within the cortical areas, the synaptic weights of the thalamocortical connections were changed.

The ensuing neuronal dynamics were analyzed using the cross correlation function between the time series in area one and two minus the shift predictor (Nowak, Munk, Nelson, James & Bullier, 1995), using 0.5 ms time steps. When analyzing the data, we used the time-series of the mean membrane potential per millisecond in each cortical area. We ran the model for 2 s of simulated time, eight times. The cross correlation between the first time series

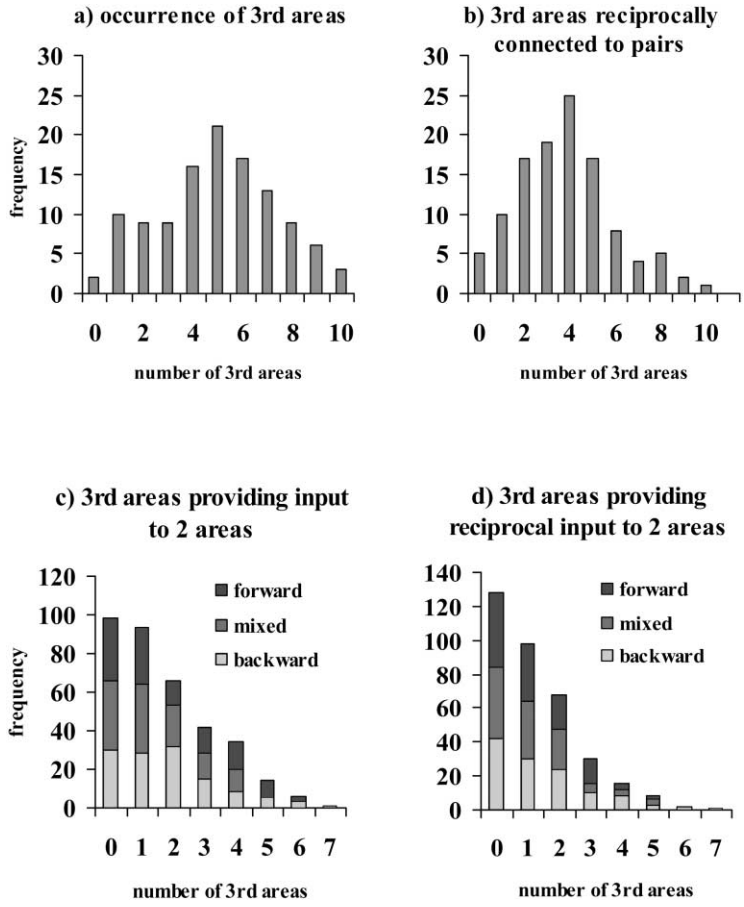

Fig. 2. (a) Histogram of how many pairs of visual areas (plotted vertically) receive common input of any type (plotted horizontally) from any number of common third areas regardless of whether the coupled areas also send input to the third areas. (b) Histogram of how many pairs of areas receive input from common third areas, that are reciprocally connected to each of the two areas. (c) Histogram of how many pairs of reciprocally connected areas receive common feedback, common feedforward and a mix of feedforward and feedback input from different numbers of common third areas, regardless of whether the coupled areas also send input to the third areas that are reciprocally connected to each of the two areas. (d) Histogram of how many sets of reciprocally connected areas receive common feedback, feedforward and a mix of feedforward and feedback input from common third areas that are reciprocally connected to each of the two areas.

(eight runs in order) and the second time series constituting eight runs in a random order constituted our shift predictor. The shift predictor reflects phase-locking due only to transients locked to the simulation onset.

3. Results

3.1. Connectivity analysis

A fundamental feature of cortical organization is the reciprocal nature of connections between cortical areas. Whereas possible functional implications of this reciprocal connectivity have been investigated extensively, little is known about the frequency with which higher order connectional topologies occur. To address this issue, we considered the frequency with which interconnectivity involving sets of three areas occur in macaque monkey visual cortex. According to the connectivity matrix of Felleman and van Essen (1991), there are 118 pairs of reciprocally connected areas in the Macaque visual cortex. Of these 118 pairs, 116 receive common projections from one or more third areas [Fig. 2(a)]. Of the latter, 113 also project back to at least one of the third areas [Fig. 2(b)]. In turn, of all the third areas that project to pairs of reciprocally connected areas, 72% receive input from the paired areas. Fig. 2(c) shows how many coupled areas receive common feedback, common feedforward and both feedback and feedforward input from one or more third areas. Fig. 2(d) shows how many of the coupled areas are reciprocally connected to common areas that provide common feedback, common feedforward and a mix of feedback and feedforward input. Overall, of the 32 visual areas included in the connectivity matrix, 29 belong to a pair of reciprocally connected areas and 26 belong to at least one triplet of reciprocally interconnected areas.

Next, we looked at the triplet architectures in relation to the experimental evidence of zero-lag between visual areas 7 and 17 in the cat visual cortex (Roelfsema et al., 1997). According to the cat connectivity matrix of Scannell, Blakemore and Young (1995), visual area 7 is much higher in the

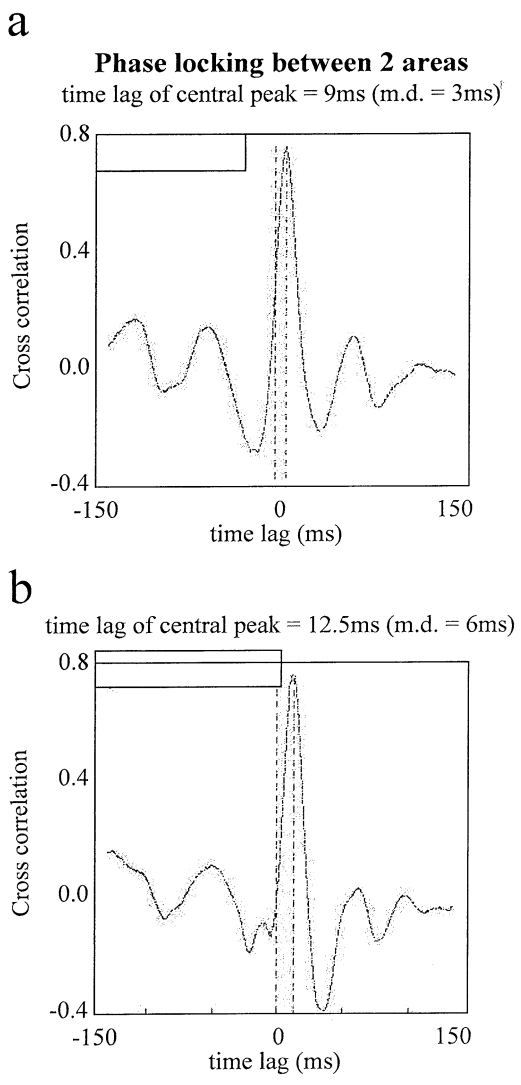

Fig. 3. Cross-correlogram functions between the average membrane potential time series from the supragranular layers of each reciprocally connected cortical area with no common third area. (a) Mean transmission delay between the two areas is 3 ms. (b) Mean transmission delay between the two areas is 6 ms.

cortical hierarchy than area 17. These areas are reciprocally connected and receive common input from 6 areas, areas 18, 19, 20a, 21a, 21b and the postero lateral suprasylvian area (Scannell et al., 1995). All of these areas are midway in the cortical hierarchy between area 17 and area 7 and so would provide feedforward input to area 7 and feedback input to area 17. Further, all of these areas receive input from areas 7 and 17.

3.2. Simulations

The first step in our simulations was to characterise the neuronal dynamics within the thalamo–cortical module. Consistent with empirical observations, both increases in cortical neuronal firing rates and the fast synchronous dynamics (characterized by the peak value of the cross-correlogram between cortical cells) were seen in response to input stimulation of the thalamus.

The next step in our simulations was to characterise the dynamics between two interconnected cortical areas, each one being composed of three layers and interacting with a thalamic region. We first considered the situation where the inter-area connections were limited to feedforward projections from one cortical area to the other. Simulations of this model failed to produce zero-lag synchrony. Next, we observed how the time lag of synchrony changed after addition of feedback connections from the upper cortical area to the lower cortical area. Adding these modulatory feedback connections did not significantly alter the time-lags between activities in the two areas (Fig. 3). In contrast, these time lags showed clear dependence on the transmission delays incurred in inter-area connections. When the mean inter-area transmission delay was 3 ms, the time-lag of the inter-area synchrony was 8 ms [Fig. 3(a)]. This lag increased to 12.5 ms for a mean inter-area transmission delay of 6 ms [Fig. 3(b)].

To explore the effects of three-way interactions on the functional coupling between cortical areas, we incorporated a third area in the model, that provided common input to the coupled areas, but did not receive input from these areas. We found that when this third area provided either feedback modulatory input to the pair of areas or feedback to one and feedforward input to the other area, the time-lag between their activities was affected in a way that depended on overall activity levels. We observed that, in our model, there was a critical activity level in the two interacting populations that was required for common modulatory inputs to become effective in reducing the time-lag of synchronous dynamics. This was between 12 and 18 spikes per second per neuron [Fig. 4(e)]. For a mean activity level in the two cortical areas below the critical level, the feedback connections were ineffective in modulating the time-lag of synchrony [Fig. 4(a)]. However, near zero phase-locking emerged when the mean activity in the two areas was above the threshold and the transmission delays between each area and the third area were equal [Fig. 4(c)]. When the mean transmission delays between the third area and each of the paired areas were different, the time-lag of synchronization was not modulated to the same extent [Fig. 4(c)], although it was slightly smaller than that incurred in the absence of the third area. This phenomena was observed both when the third area provided feedback modulatory input to cortical pair and when the third area was modeled as being intermediate in the cortical hierarchy, thereby providing feedback to one area and feedforward to the other.

The fourth and final architecture that we considered included reciprocal connections between the third area and the coupled areas. Once again, when this third area provided either feedback modulatory input to the pair of

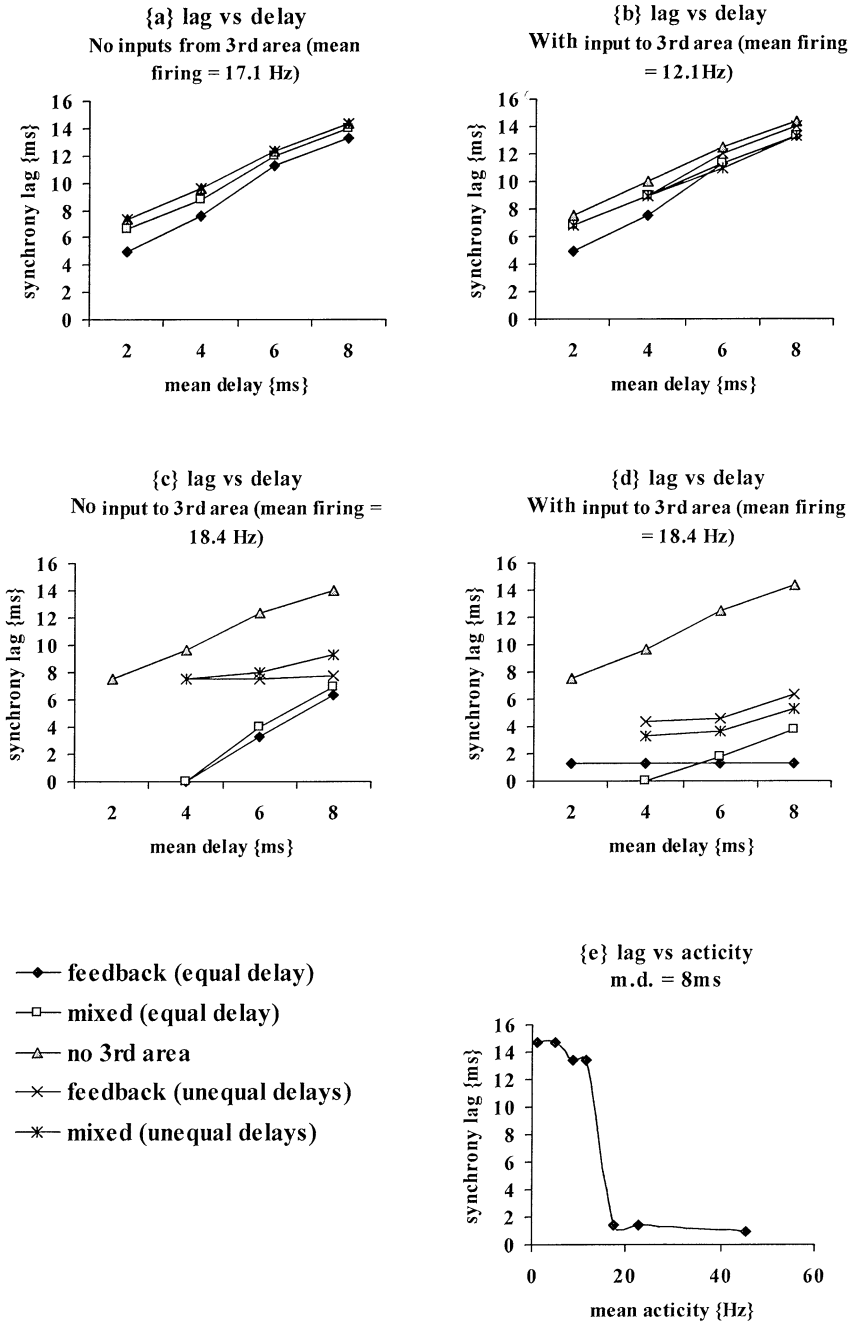

Fig. 4. Graphs plotting the time-lag of the central peak in the cross-correlogram against the mean extrinsic transmission delays when a third area is now added to the paired cortical areas. (a) Shows cases where the third area provides common feedback or a mixture of feedforward and feedback input with the same or different mean transmission delays to the coupled areas and the paired areas do not reciprocate their connections. (b) Shows cases where the third area provides common feedback or a mixture of feedforward and feedback input to the paired areas, with equal or differential mean transmission delays and the coupled areas do reciprocate these connections. In (a) and (b), the mean cell spiking rate in the cortical areas, before the addition of the third areas was 12.1 Hz. (c), (d) Shows the same as (a) and (b), except that now, the mean activity level was 18.4 Hz. (e) Time-lag of the central peak in the cross-correlogram between the two paired areas, with a third area providing common feedback input that is reciprocated by the coupled areas, plotted against mean spiking rate across both areas. The mean transmission delay between the two areas in this case was 8 ms.

areas or feedback to one and feedforward to the other, modulation of the time-lag of inter-area synchrony was minimal if the activity level in the areas was below around 15 Hz [Fig. 4(b)]. However, when the mean cortical activity level was above this level and the third area provided weak modulatory input to the paired cortical areas, the time lag of phase-locking between areas approached zero [Fig. 4(d)], regardless of the mean differential transmission delays between the third area and the paired areas. Similarly, when the third area provided driving feedforward input to

one of the paired areas and modulatory feedback to the other, the phase-locking was again modulated to near zero time-lag [Fig. 4(d)].

4. Discussion

The phenomenon of zero-lag synchrony between activities spread across different levels of a cortical hierarchy is intriguing because it is not immediately clear what mechanisms are capable of supporting it. The question that this work addressed was 'what is the minimum sufficient cortical architecture that will support zero phase lag synchronization between two cortical areas?'. Results showed that reciprocal connections between pairs of areas located at different levels in a sensory hierarchy were not sufficient to account for the zero phase locking of their activities. However, as long as the intrinsic activity within the cortical areas was not too low, common modulatory input from a third area substantially brought down the time-lag of synchronization. Further, we found that non-reciprocal connections from a third area to each coupled area may not be sufficient for zero phase-lag synchrony [Fig. 4(c)] when the transmission delays between each coupled area and the third area are significantly different. This suggests that for the time-lag of phase-locking to be reduced, the third area must be reciprocally connected to each coupled area. In this architecture, the phase-lag among areas is reduced through the dynamic and reciprocal interplay between all three components of the triad. Empirical observations of zero-lag synchrony are consistent with the anatomical evidence that a high proportion (96%) of all coupled areas in the cortex of the cat are reciprocally connected to a third area (Fig. 2), thus forming triplets of mutually interacting cortical regions. It must also be noted that, although this paper focused on how common inputs from a third cortical area reduce the time-lag of inter-cortical synchrony, there is also the possibility that thalamocortical projections may mediate this effect. For example, the LP-pulvinar feeds common input into primary and secondary visual areas (Kato, 1990), which may account for the near-zero synchrony observed between V1 and V2 neurons in the monkey (Frien et al., 1994).

It was found from analyzing the experimental literature (Felleman and Van Essen, 1991) that most visual areas receive common input from a third area, where the common input is equally likely to be feedforward, feedback or a mixture of feedforward and feedback. Thus, when taking an example of empirically-observed zero-lag synchrony between two visual areas (Roelfsema et al., 1997), we noted on the basis of known neuroanatomy that these two areas receive a mixture of feedforward and feedback input from a number of third cortical areas. The finding that common feedback projections from a third area provides a potent mechanism for synchronization is significant, as it can account for the zero-lag synchrony between areas at the early stages of the sensory hierarchy. The potential of feedback connections to induce inter-regional synchronization is reinforced by anatomical considerations. Ascending efferents target only a very small cortical volume, the chances of these connections being to cells that have been measured electrophysiologically are very small. Conversely, feedback connections are more widespread and are more likely to impinge on two units or populations in lower cortical areas. According to the literature, ascending input has been shown to use the type of synaptic arbors that are round and dense while descending connections have extended arbors that are much sparser. Round arbors embody around 100 terminals over an area of diameter of about 100 μm while extended arbors incorporate roughly 500–1000 terminals over an area of diameter, 1–3 mm (Crick and Koch, 1998; Rockland, 1996). Therefore, as feedback connections cover a much larger cortical volume than feedforward inputs, they are more likely to modulate synchronous interactions over two units or populations picked at random.

In this study, we investigated the role of triplets of cortical areas in mediating inter-areal synchronous interactions. Such synchronous dynamics are thought to constitute a form of temporal coding that underlies feature binding and perceptual synthesis. In this way, the binding of different features of an object may be accomplished, in the temporal domain, through the transient synchronization of oscillatory responses (Milner, 1974; von der Malsburg, 1981; Sporns, Tononi & Edelman, 1990). Indeed, synchronization in the visual cortex appears to depend on stimulus properties such as continuity, orientation similarity and motion coherency (Gray, Konig, Engel & Singer, 1989; Engel, Konig, Kreiter, Gray & Singer, 1990; Freiwald, Kreiter & Singer, 1995). Although, this study did not explicitly address the role of synchrony in mediating such functional integration, our results suggest that the organisation of cortical areas into triplets provides a basic framework for functional integration, from which pattern specific temporal codes can be expressed.

Acknowledgements

This work was supported by the Wellcome Trust.

Appendix A. Modelling neuronal dynamics

The instantaneous change in membrane potential of each model neuron, $V(t)$, was given by:

$$\tau_{\mathrm{m}} \frac{\partial V}{\partial t} = -V + V_0 - \sum_j g_j(V - V_j)$$

where τ_m is a passive membrane time constant set at 16 ms (8 ms) for cortical excitatory (inhibitory) cells and the sum on the right hand side is over synaptic currents. V_0 denotes

Table 2
The parameter values of the model

Receptor	g_{peak} (mS)	τ_1 (ms)	τ_2 (ms)	V_j (mV)
AMPA	0.05	0.5	2.4	0
GABAa	0.175	1	7	−70
GABAb	0.0017	30–90	170–230	−90
NMDA	0.01	0	100	0

the passive resting potential that was set to a value of −60 mV. V_j are the equilibrium potentials for the j-th synaptic type. V was reset to the potassium reversal potential of −90 mV, when it exceeded a threshold of −50 mV and a spike event was generated for that unit. Synaptic activations of AMPA, GABAa and GABAb receptors were expressed as a change in the appropriate channel conductance, g_j, according to a dual exponential response to single spike events in afferent neurons given by:

$$g = g_{\text{peak}} \frac{\exp(-t/\tau_1) - \exp(-t/\tau_2)}{\exp(-t_{\text{peak}}/\tau_1) - \exp(-t_{\text{peak}}/\tau_2)}$$

τ_1 and τ_2 are the rise and decay time constants, respectively, and t_{peak}, the time to peak. $g = t_{\text{peak}} = \tau_1\tau_2/(\tau_1 - \tau_2)$. g_{peak} represents the maximum conductance for any particular receptor.

Conductances were implicitly normalized by a leak membrane conductance, so that they were dimensional. The implementation of NMDA channels, was based on Traub, Wong, Miles and Michelson (1991):

$$I_{\text{NMDA}} = g_{\text{NMDA}} M(V - V_{\text{NMDA}})$$

$$\frac{\partial g_{\text{NMDA}}}{\partial t} = -\frac{g_{\text{NMDA}}}{\tau_2}$$

$$M = \frac{1}{1 + (\text{Mg}^{2+}/3)\exp(-0.07(V - \xi)}$$

I_{NMDA} is the current that enters linearly into the equation for $\partial V/\partial t$ above. g_{NMDA} is a ligand-gated virtual conductance. M is a modulatory term that mimics the voltage-dependent affinity of the Mg^{2+} channel pore. ξ is −10 mV and Mg^{2+} is the external concentration of Mg^{2+} often used in hippocampal slice experiments (2 mM). These and other parameters (Table 2) were consistent with experimental data (see Lumer et al., 1997a for details).

References

Beaulieu, C., & Colonnier, M. (1983). The number of neurons in the different laminae of the binocular and monocular regions of area 17 in the cat. *J. Comp. Neurology*, *217*, 337–344.

Beaulieu, C., & Colonnier, M. (1985). A laminar analysis of the number of round-asymmetrical and flat-symmetrical synapses on spines, dendritic trunks and cell bodies in area 17 of the cat. *J. Comp. Neurology*, *231*, 180–189.

Beaulieu, C., Kisvarday, Z., Somogyi, P., & Cynader, M. (1992). Quantitative distribution of GABA -immunopositive and -immunonegative neurons and synapses in the monkey striate cortex (area 17). *Cerebral Cortex*, *2*, 295–309.

Calabresi, P., Mercuri, N. B., Stefani, A., & Bernardi, G. (1990). Synaptic and intrinsic control of membrane excitability of neostriatal neurons—I: an in vivo analysis. *J. Neurophysiol.*, *63* (2), 651–662.

Crick, F., & Koch, C. (1998). Constraints on cortical and thalamic projections: the no-strong loops hypothesis. *Nature*, *391*, 245–250.

Engel, A. K., Konig, P., Kreiter, A. K., Gray, C. M., & Singer, W. (1990). Temporal Coding by coherent oscillations as a potential solution to the binding problem. *Nonlinear Dynamics and Neural Networks, VCH*, *3*, 26.

Felleman, D. J., & Van Essen, D. C. (1991). Distributed hierarchical processing in the primate cerebral cortex. *Cerebral Cortex*, *1*, 1–47.

Freiwald, W. A., Kreiter, A. K., & Singer, W. (1995). Stimulus dependent intercolumnar synchronization of single unit responses in cat area 17. *NeuroReport*, *6*, 2348–2352.

Frien, A., Elkhorn, R., Bauer, R., Wellborn, T., & Kr, H. (1994). Stimulus-specific fast oscillations at zero phase between visual areas V1 and V2 of awake monkey. *NeuroReport*, *5*, 2273–2277.

Friston, K. J., Ungerleider, L. G., Jezzard, P., & Turner, R. (1995). Characterizing modulatory interactions between areas V1 and V2 in human cortex: a new treatment of functional MRI data. *Human Brain Mapping*, *2*, 211–224.

Kato, N. (1990). Cortico–thalamo–cortical projection between visual cortices. *Brain Res.*, *509*, 150–152.

Girard, P., & Bullier, J. (1989). Visual activity in area V2 during reversible inactivation of area 17 in the macaque monkey. *J. Neurophysiol.*, *62*, 1287–1301.

Gray, C. M., Konig, P., Engel, A. K., & Singer, W. (1989). Oscillatory responses in cat visual cortex exhibit inter-columnar synchronization which reflects global stimulus properties. *Nature*, *338*, 334–337.

Lorenzon, N. M., & Foehring, R. C. (1992). Relationship between repetitive firing and afterhyperpolarizations in human neocortical neurons. *J. Neurophysiol.*, *67* (2), 350–363.

Lumer, E. D., Edelman, G. M., & Tononi, G. (1997a). Neural dynamics in a model of the thalamocortical system—I: layers, loops and the emergence of fast synchronous rhythms. *Cerebral Cortex*, *7*, 207–227.

Lumer, E. D., Edelman, G. M., & Tononi, G. (1997b). Neural Dynamics in a model of the thalamocortical System—II: the role of neural synchrony tested through perturbations of spike timing. *Cerebral Cortex*, *7*, 228–236.

Milner, P. M. (1974). A model for visual shape recognition. *Psychological Review*, *81* (6), 521–535.

Nicolelis, M. A. L., Baccala, L. A., Lin, R. C., & Chapin, J. K. (1995). Sensorimotor encoding by synchronous neural ensemble activity at multiple levels of the somatosensory system. *Science*, *268*, 1353–1358.

Nowak, L. G., Munk, M. H., Nelson, J. I., James, A. C., & Bullier, J. (1995). Structural basis of cortical synchronization—I: three types of interhemispheric coupling. *Neurophys.*, *76*, 1–22.

Otis, T., & Mody, I. (1992). Differential activation of GABAa and GABAb receptors by spontaneously released transmitter. *J. Neurophysiol.*, *67*, 227–235.

Otis, T., Konick, Y. D., & Mody, I. (1993). Characterization of synoptically elicited GABAb responses using patch-clamp recordings in rat hippocampal slices. *J. Physiol. London*, *463*, 391–407.

Rockland, K. S. (1996). Two types of corticopulvinar terminations: round (type 2) and elongate (type 1). *J. Comp. Neurol.*, *368*, 57–87.

Roelfsema, P. R., Engel, A. K., Konig, P., & Singer, W. (1997). Visuomotor integration is associated with zero time-lag synchronization among cortical areas. *Nature*, *385*, 157–161.

Sandell, J. H., & Schiller, P. H. (1982). Effect of cooling area 18 on striate cortex cells in the squirrel monkey. *J. Neurophysiol.*, *48*, 38–48.

Scannell, J. W., Blakemore, C., & Young, M. P. (1995). Analysis of

connectivity in cat cerebral cortex. *Journal of Neurosci.*, *15* (2), 1463–1483.

Schiller, P. H., & Malpeli, J. G. (1977). The effect of striate cortex cooling on area 18 cells in the monkey. *Brain Res.*, *126*, 366–369.

Sporns, O., Tononi, G., & Edelman, G. M. (1990). Dynamic interactions of neuronal groups and the problem of cortical integration. *Nonlinear Dynamics and Neural Networks, VCH*, 205–240.

Stern, P., Edwards, F., & Sakmann, B. (1992). Fast and slow components of unitary epsps on stellate cells elicited by focal stimulation in slices of rat visual cortex. *J. Physiol. London*, *449*, 247–278.

Sukov, W., & Barth, D. S. (1998). Three-dimensional analysis of spontaneous and thalamically evoked gamma oscillations in auditory cortex. *J. Neurophysiol.*, *79* (6), 2875–2884.

Traub, R. D., Wong, R. K., Miles, R., & Michelson, H. (1991). A model of a CA3 hippocampal pyramidal neuron incorporating voltage-clamp data on intrinsic conductances. *J. Neurophysiol.*, *66*, 635–650.

von der Malsburg C. (1981). *The correlation theory of the brain*. Internal report Max Planck Institute for Biophysical Chemistry, Gottingen, West Germany.